

**Currents and waves
in the northern Gulf of
Riga: measurement and
long-term hindcast***

doi:10.5697/oc.54-3.421
OCEANOLOGIA, 54 (3), 2012.
pp. 421–447.

© *Copyright by
Polish Academy of Sciences,
Institute of Oceanology,
2012.*

KEYWORDS

Hydrodynamic modelling
Water exchange
Wave hindcast
Wind climate
RDCP
Baltic Sea

ÜLO SUURSAAR*
TIIT KULLAS
ROBERT APS

Estonian Marine Institute,
University of Tartu,
Mäealuse 14, EE–12618 Tallinn, Estonia;

e-mail: ulo.suursaar@ut.ee

*corresponding author

Received 27 February 2012, revised 19 April 2012, accepted 30 April 2012.

Abstract

Based on measurements of waves and currents obtained for a period of 302 days with a bottom-mounted RDCP (Recording Doppler Current Profiler) at two differently exposed locations, a model for significant wave height was calibrated separately for those locations; in addition, the Gulf of Riga-Väinameri 2D model was validated, and the hydrodynamic conditions were studied. Using wind forcing data from the Kihnu meteorological station, a set of current, water exchange and wave hindcasts were obtained for the period 1966–2011. Current patterns in the Gulf and in the straits were wind-dependent with characteristic wind switch directions. The Matsi coast was prone to upwelling in persistent northerly wind conditions. During the

* The study was supported by the Estonian target financed project 0104s08, the Estonian Science Foundation grant No 8980 and by the EstKliima project of the European Regional Fund programme No 3.2.0802.11-0043.

The complete text of the paper is available at <http://www.iopan.gda.pl/oceanologia/>

hindcast period, currents increased along the Kõiguste coast and in the Suur Strait, waves decreased noticeably off Kõiguste but fluctuated without a clear linear trend near Matsi. The spatially contrasting results for differently exposed coasts were related to the corresponding variations in local wind conditions and to changes in atmospheric circulation patterns over northern Europe.

1. Introduction

Hydrodynamic processes are the main agents that alter the concentrations and spatial distributions of biologically important nutrients and water column properties in nearshore marine areas. Causing direct physical disturbances, turbidity and resuspension of bottom sediments, orbital motions due to surface waves and other sea level fluctuations influence bottom life down to depths of approximately 10–20 m (Jönsson 2006, Kovtun et al. 2011). The impact is especially strong around the shoreline, where hydrodynamically forced geomorphic processes redistribute sediment and shape the coast (e.g. Tõnisson et al. 2008). In the regions of straits and estuaries, currents also have a special importance because of their association with matter exchange processes and frontal movements (e.g. Bowman & Esaias (eds.) 1978, Astok et al. 1999).

This study focuses on the northern Gulf of Riga and the adjoining small sub-basin called the West Estonian Archipelago Sea (or the Moon-sund, Väinameri). Influenced by the large freshwater and nutrient inflow from rivers, these semi-enclosed, relatively productive and shallow water-bodies have attracted considerable attention, e.g. from marine biologists. A number of publications dealing both with basin-wide problems of the Gulf (e.g. Berzinsh et al. 1994, Ojaveer 1995), as well as some locally focused papers, call for a better understanding of the hydrodynamic variability in the changing climate and increasing anthropogenic pressure (Kotta et al. 2008). In terms of scientific effort and the number of publications, Kõiguste Bay (where a marine biology field station is located) on the south-eastern coast of Saaremaa Island and the Suur Strait (Figure 1) are prominent. Considered to be one of the key outlets in the exchange of matter between the Gulf of Riga and the relatively less polluted Baltic Proper, the Suur Strait is where the first extensive measurement series of currents were carried out in the 1990s (Suursaar et al. 1995, Astok et al. 1999). Based on hydrodynamic models, currents and matter exchange were modelled by Otsmann et al. (1997, 2001), Suursaar & Kullas (2006) and Raudsepp et al. (2011). Some of the studies were motivated by plans to build a fixed link (a series of bridges and road dams) across the strait from the Estonian mainland to Saaremaa Island. However, after more than ten years of

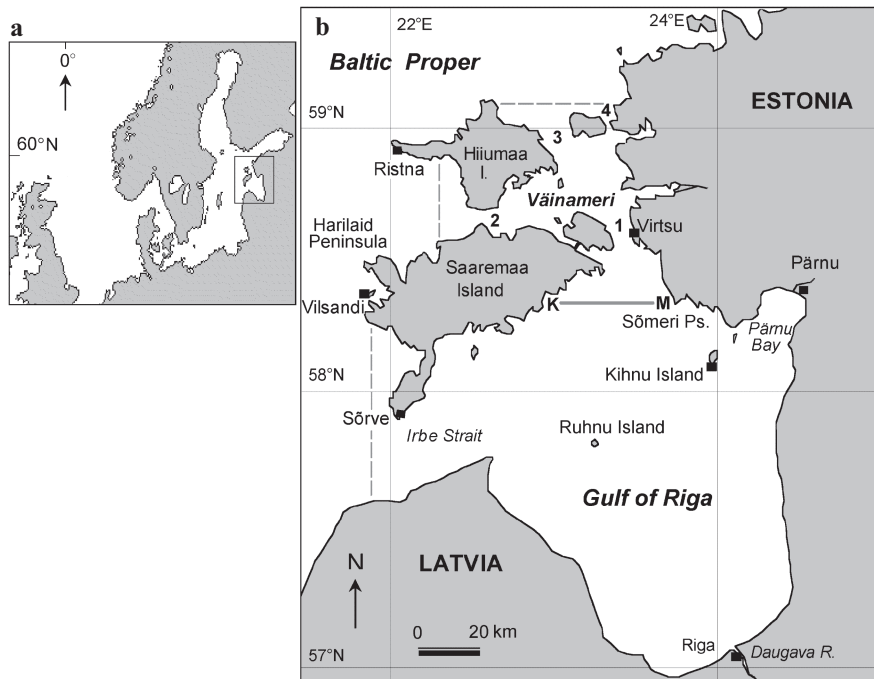


Figure 1. Map of the study area. The RDCP mooring and subsequent hydrodynamic modelling locations at Kõiguste (K) and Matsi (M) together with the longitudinal section between them is shown. The open boundaries of the Gulf of Riga – Väinameri 2D hydrodynamic model (dashed line). The Straits of the Väinameri: Suur Strait (1), Soela Strait (2), Hari Strait (3) and Voosi Strait (4)

cost-benefit studies and environmental impact assessments, the project is still pending.

This paper stems mainly from a series of oceanographic measurements performed using a bottom-mounted Recording Doppler Current Profiler (RDCP) at sites near the entrance to the Kõiguste Bay and Matsi (Figure 1). Besides the single-point current measurements in the Suur Strait in 1993–1996 (630 days by Otsmann et al. 2001) and in 2008 (21 days by Raudsepp et al. 2011), the multi-layer measurements at Kõiguste (221 days in October 2010–May 2011) and Matsi (81 days in June–September 2011) are the most extensive hydrodynamic measurements ever to have been made in the northern Gulf of Riga. The aims of the paper are: (1) to present selected measurement data regarding currents and waves; (2) to use the measurements as a calibration reference for a fetch-based wave model and a validation source for a hydrodynamic model, and to reconstruct wave parameters and currents at selected locations for the period 1966–2011; and

(3) to discuss decadal changes in the water exchange and wave climate of our study area together with variations in the wind climate.

2. Material and methods

2.1. Study area and measurements

Although the in situ measurements were concentrated in the northern part of the Gulf of Riga, the hydrodynamic conditions and water exchange depends on the morphometric features of the Gulf as a whole. Moreover, an indispensable prerequisite for a successful modelling study is the distinctive semi-enclosed shape of the basin and the relatively short open boundaries to be used in the model. The Gulf of Riga measures roughly 140×150 km² and has a surface area of 17 913 km². The Väinameri is approximately 50×50 km², with a surface area of 2243 km². The maximum depth of the Gulf is 52 m and the average depth is 23 m. The Väinameri is even shallower with an average depth of 4.7 m. The sub-basins are connected to each other through the nearly meridional Suur Strait, and with the Baltic Proper by four straits lying in the SW (Irbe Strait), W (Soela Strait) and NW (Hari and Voosi Strait) directions. Functioning together as an intricate oscillatory system, all the straits take part in the water exchange processes (Otsmann et al. 2001). The Irbe Strait, the largest one, is 27 km wide. The Suur Strait has a width of 5 km, a maximum depth of 20 m and a cross-sectional area of 0.044 km². The Hari, Voosi and Soela Straits are 8, 2 and 4 km wide respectively.

Annually, the Gulf receives some 32 km³ of freshwater input from rivers (mainly from the Daugava in the southern part of the Gulf), while the Väinameri receives 1 km³ yr⁻¹ on average. The average salinity in the Gulf of Riga is approximately 5.6 (Berzinsh et al. 1994) and the salinity in the Baltic Proper near the Gulf is 7.2. Because of its shallowness, the absence of significant density gradients between the sub-basins, and weak tides, the major factors forcing water exchange are wind stress and occasional sea level differences (which are also mainly produced by wind conditions).

The maximum depth along the longitudinal transect between the Kõiguste and Matsi measuring sites is 24 m (Figure 1). North of that 23 km long transect begins the funnel-like entrance to the Suur Strait with typical depths between 5 and 15 m. A self-contained medium-range (600 Mhz) oceanographic instrument RDCP-600 manufactured by Aanderaa Data Instruments (AADI) was deployed by divers on the seabed at 58°19.2'N 23°01.2'E (Kõiguste), about 4 km offshore. The upward-facing instrument

was deployed for the period 2 October 2010–11 May 2011, and 5310 hours of multi-layer current data were obtained. The same instrument was used for recording at the Matsi site (58°20.4'N 23°42.8'E, 1.5 km off the Sõmeri Peninsula) from 1400 hrs GMT on 13 June 2011. As at Kõiguste, the measuring interval was set at 1 hour and the instrument provided 1941 hours of data until 2 September 2011. The RDCP-600 was also equipped with some additional sensors to measure temperature, conductivity, oxygen and turbidity. The high accuracy quartz-based pressure sensor (resolution 0.001% of full scale) was used to measure the waves above the instrument. The significant wave height H_s , the most commonly used wave parameter, was calculated from the energy spectrum. It represents the average height of the 1/3 highest waves, and is roughly equal to the visually observed 'average wave height'.

The initial mooring depth was about 12 m at Kõiguste and 10 m at Matsi but the instantaneous water depth varied in time with meteorologically driven sea level changes (Figure 2a,b). The vertical column set-up for flow measurements included a 2 m cell size with a 50% overlap, so the '3 m depth' actually represented the 2–4 m depth interval etc. Beginning with the seabed, there was a 2 m blank distance between the instrument and the lowest measurable cell. Moreover, depending on sea level variations and wave heights, the measurements within the uppermost 1–3 metres were discarded because of high standard deviations. Thus, 6 depth layers covering the 2–9 m depth range were normally monitored.

In order to obtain information on near-bottom velocities, additional measurements were taken at Matsi between 13 and 17 June 2011 using a short range 3 MHz Acoustic Doppler Profiler (ADP) (YSI/Sontek). The instrument was deployed approximately 0.5 km shorewards of the RDCP at 8 m depth. With a 20 cm cell size, the profiles with a 4 min time step were started 0.7 m from the bottom. At the location between RDCP and ADP deployments, a Lagrangian surface float (kindly supplied by Dr Tarmo Kõuts of the Marine Systems Institute, Tallinn Technical University) was released simultaneously, which transmitted hourly coordinates.

After its release, the float started to recede to the SSE. The data transmitted during the first one-two hours can be used for estimating the surface velocities at Matsi at that time.

2.2. Models and forcing data

Although the same RDCP measurements were used for the calibration-validation of both wave and current models, quite different approaches were required for their hindcast. For currents and water exchange, we used a two-dimensional (2D) hydrodynamic model. The shallow sea depth-averaged

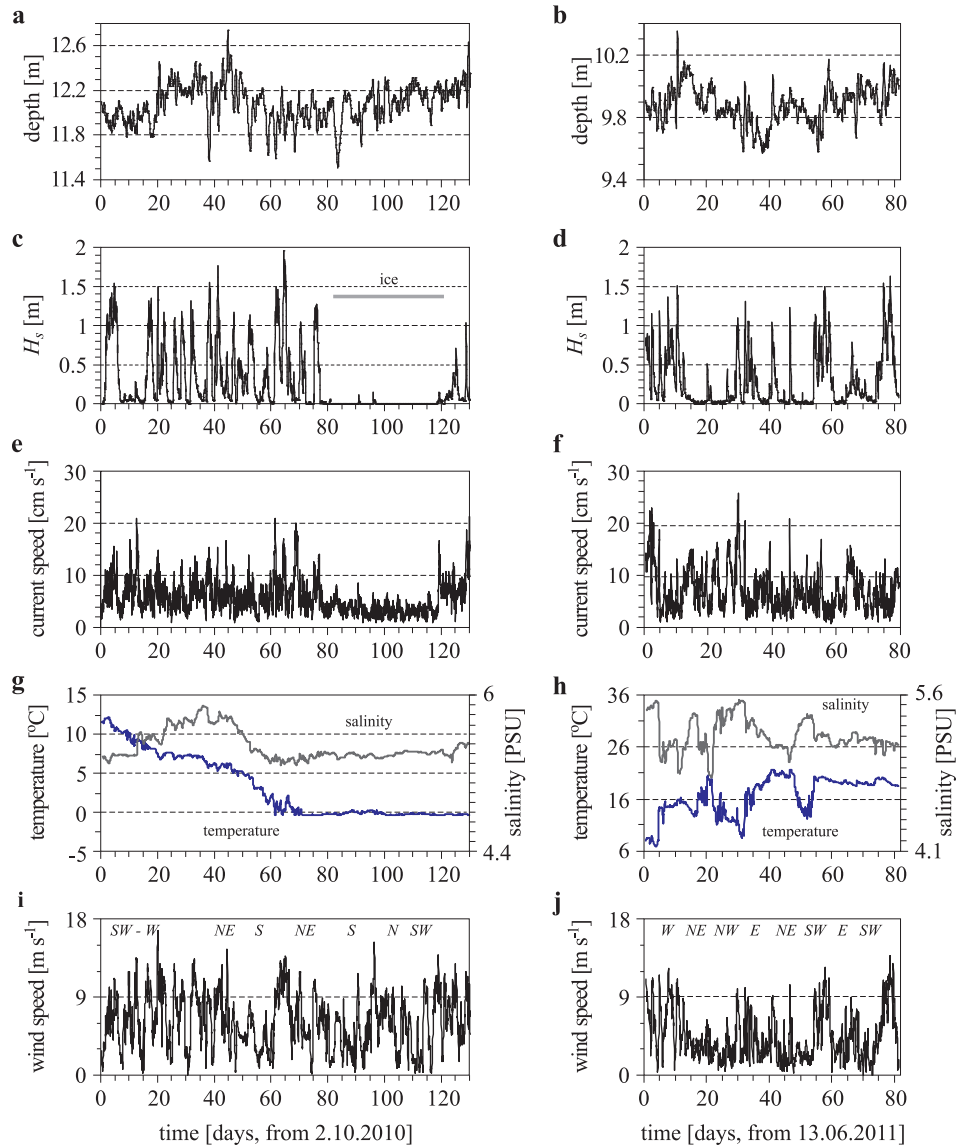


Figure 2. Time series of measurements at Kõiguste (left-hand panel, 130 days excerpt) and at Matsi (right panel): sea level variations (a,b), wave heights (c,d), vertically integrated (2–9 m from the bottom) current speed modula (e,f), water temperature and salinity (g,h); wind speed modula (together with prevailing wind directions marked above the graphs) measured at Kihnu station for the same periods (i,j)

free-surface model with quadratic bottom friction consists of momentum balance and volume conservation equations:

$$\frac{DU}{Dt} - fV = -g(H + \xi)\frac{\partial\xi}{\partial x} + \frac{\tau_x}{\rho_w} - \frac{kU}{H^2}(U^2 + V^2)^{1/2}, \quad (1)$$

$$\frac{DV}{Dt} + fU = -g(H + \xi)\frac{\partial\xi}{\partial y} + \frac{\tau_y}{\rho_w} - \frac{kV}{H^2}(U^2 + V^2)^{1/2}, \quad (2)$$

$$\frac{\partial\xi}{\partial t} + \frac{\partial U}{\partial x} + \frac{\partial V}{\partial y} = 0, \quad (3)$$

$$\frac{D}{Dt} = \frac{\partial}{\partial t} + \frac{1}{H} \left(U \frac{\partial}{\partial x} + V \frac{\partial}{\partial y} \right), \quad (4)$$

where U and V are the vertically integrated volume flows in the x and y directions respectively, ξ is the sea surface elevation as the deviation from the equilibrium depth (H), f is the Coriolis parameter, ρ_w is the water density, k is the bottom frictional parameter ($k = 0.0025$, e.g. Jones & Davies 2001), and τ_x and τ_y are wind stress ($\vec{\tau}$) components along the x and y axes. Wind stress ($\vec{\tau}$) was computed using the formula by Smith & Banke (1975):

$$\vec{\tau} = \rho_a C_D |\vec{W}_{10}| \vec{W}_{10}, \quad (5)$$

which includes a non-dimensional empirical function of the wind velocity:

$$C_D = (0.63 + 0.066 |\vec{W}_{10}|) 10^{-3}, \quad (6)$$

where $|\vec{W}_{10}|$ is the wind velocity vector modulus [m s^{-1}] at 10 m above sea level and ρ_a is the air density. The model simulates both sea level and current values depending on local wind stress and open boundary sea level forcing. The model domain encompasses the entire areas of the Gulf of Riga and the Väänameri sub-basins with a model grid of horizontal resolution of 1 km, yielding a total of 18 964 marine grid-points (including 2510 in the Väänameri). A staggered Arakawa C grid is used with the positions of the sea levels at the centre of the grid box and the velocities at the interfaces. At the coastal boundaries the normal component of the depth mean current is taken to be zero. In response to variations in sea level, wetting and drying are not included. A minimum depth of 0.5 m is imposed for sea level variations at the sea points and at coastal borders, but sea level can increase freely. Allowing fluxes through it, the model has short open boundaries, which are shifted by 5–20 km outside the narrowest parts of the straits. The model equations were solved numerically using the finite difference method with an integration time step of 30 seconds. Because of the chosen time step and horizontal grid resolution, the numerical diffusion generated by the numerical scheme was relatively low.

The 2D model performance had earlier been compared with a Helmholtz-type model (Otsmann et al. 2001) and flow measurements in the straits from 1993 to 1995 (Kullas et al. 2000). Hindcast simulations for 1999 and 2005 proved the model's success in simulating sea level (Suursaar et al. 2002, 2006). Outside the straits, in situ flow measurements for model comparison were not available until this study.

Although some gridded geostrophic wind or re-analysis data are in principle available, including the latest ERA-40 refinement for the Baltic Sea area known as BaltAn65+ (Luhamaa et al. 2011), such data cannot be used in this study for meteorological forcing. Covering 1965–2005 with a 6 h time step, the BaltAn65+ does not match our measurements from 2011. We used hourly wind and sea level time series measured by the Estonian Meteorological and Hydrological Institute (EMHI). Obtained from the Ristna tide gauge, which is located just outside the Soela Strait (Figure 1), the hourly sea level data were applied in identical fashion at the four cuts of the open boundaries. The wind stress was calculated from the wind data measured at the Kihnu meteorological station, located at the southern tip of Kihnu Island. Although the Virtsu station is somewhat closer to both measuring sites, it lies in a far more sheltered position, and unlike Kihnu, it does not adequately represent marine winds (Keevallik et al. 2007). A spatially homogeneous wind was applied at the grid-points. The one-hour sustained wind speed data had a 1 h time step.

Although the Kihnu station has been operational since 1931, EMHI digitized wind data have been available only since 1966. The completeness of the data set is very good. The time interval of the older data (until 2003) is 3 hours, but for hydrodynamic modelling they were subsequently interpolated into an applicable format. The value step was 1 m s^{-1} until September 2003, and 0.1 m s^{-1} thereafter. Wind directions were given in the 16-rhumb system in 1966–1976 (converted into degrees in the EMHI database), the resolution was 10° until 2003, and the currently used equipment providing a 1° resolution output. Thus, with regard to the potential homogeneity issue, three sub-sets can be distinguished over the study period. Wind speed was measured with a wind vane of Wild's design during 1966–1976, a recording anemorhumbometer during 1976–2003, and the MILOS-520 automatic weather station after September 2003. While the latest change in measuring equipment in 2003 did not introduce any substantial discrepancies into the data sets according to e.g. Keevallik et al. (2007), problems may appear as a result of the change from wind vanes (weathercocks) to automatic anemorhumbometers in November 1976. Back then, some parallel measurements were performed for a few years. It turned out that the new anemorhumbometers were

systematically underestimating strong ($> 10 \text{ m s}^{-1}$) winds in comparison to the previous visual readings from the weathercocks. Therefore, during data pre-treatment, we adjusted the strong wind data from 1966–1976 with corrections provided by a professional handbook (Scientific-practical Handbook of the Climate of the USSR 1990). This procedure, which slightly reduces wind speeds over 10 m s^{-1} , was also briefly described in Suursaar & Kullas (2009). For example, a wind speed of 11 m s^{-1} corresponds to the previous 12 m s^{-1} , and 20 m s^{-1} is equivalent to the previous 23 m s^{-1} . In the case of both currents and winds, the positive direction is east for u and north for v when velocity components are used.

The same wind forcing was also used in two locally calibrated wave hindcasts in 1966–2011. The semi-empirical model version for shallow and intermediate-water waves used, also known as the significant wave method, is based on the fetch-limited equations of Sverdrup, Munk and Bretschneider. Currently such models are better known as the SPM method (after a series of Shore Protection Manuals, e.g. USACE 2002). The model version that we used is the same as the one used by Huttula (1994) and Suursaar & Kullas (2009):

$$H_s = 0.283 \frac{U^2}{g} \tanh \left[0.53 \left(\frac{gh}{U^2} \right)^{0.75} \right] \times \tanh \left\{ \frac{0.0125 \left(\frac{gF}{U^2} \right)^{0.42}}{\tanh \left[0.53 \left(\frac{gh}{U^2} \right)^{0.75} \right]} \right\}, \quad (7)$$

where the significant wave height H_s is a function of wind speed U , effective fetch length F and depth h ; U is in m s^{-1} , F and h are in m , and g is the acceleration due to gravity in m s^{-2} . No wave periods or lengths were calculated, because it is not possible to calibrate the model simultaneously with respect to H_s and wave periods. The RDCP, with a cut-off period of about 4 seconds for our mooring depth, could not provide proper calibration data for wave periods, as the RDCP and wave models represent somewhat different aspects of the wave spectrum.

This relatively simple method can deliver reasonably good and quick results for semi-enclosed medium-sized water bodies, such as big lakes (Seymour 1977, Huttula 1994). Also, in the sub-basins of the Baltic Sea the role of remotely generated waves is small and the memory time of the wave fields is relatively short (Soomere 2003, Leppäranta & Myrberg 2009). In practical applications, the main problem for such models seems to be the choice of effective fetch lengths, given the irregular coastline and bathymetry of this water body. Traditionally, fetches are prescribed as the headwind distances from the nearest shores for different wind directions, and an algorithm is applied that tries to take into account basin properties in

a wider wind sector (e.g. Massel 1996). We proposed a calibration procedure where the angular distributions of fetches are adjusted using high-quality wave measurements, so that afterwards the model can act as a ‘virtual’ extension of the fixed point measurements in hindcasts (Suursaar 2010).

For calibration, we first measured the angular distributions of fetches with a step of 20° from the nautical charts for our study locations of Kõiguste and Matsi. However, it was difficult to assess the exact influences of islands, shoals and the coastline on waves, and the comparisons of results between the measured and modelled hourly time series were not good enough. New distributions of fetches were created by maximizing the correlation coefficient and minimizing the root square error (RMSE) in the procedure, where the fetches are adjusted separately in all 20° sectors. The procedure also appears to enhance the fetches from the directions where the measured wind forcing is restricted or distorted compared to the undisturbed wind properties at the wave measuring and modelling site. The calibration results are discussed in section 3.2.

3. Results and discussion

3.1. Measurement results of currents and waves in 2010–2011

As the measuring period at Kõiguste was longer (221.2 days) than at Matsi (80.8 days), it included weather conditions over a larger range of variability. Variability ranges in sea level fluctuations measured as ‘instrument depth’ (1.23 m vs. 0.78 m, Table 1), salinity (1.18 vs. 0.83) and maximum wave heights (2.93 vs. 2.46 m) were also larger. Average properties of waves and currents at Kõiguste were somewhat influenced by sea ice (Figure 2), which covered the measuring site for the first time at the end of December 2010. For a short period in February, the whole Gulf of Riga was ice-bound and ice forms of some kind were present until the end of April.

Because of the proximity to the coast, the measured currents tended to be polarized and modified by the coastline. Especially at Matsi, most of the velocity readings lay within two narrow directional intervals of 210–350 and 140–170 degrees: the v (S-N component) described 80–90% of the total variability (Figure 3b). At Kõiguste, longshore (SW-NE) currents dominated as well, but as a result of the microfjord-like bottom topography, the directional scatter was considerably larger. Both currents and waves largely depended on wind conditions; no remarkable storm events occurred. At Matsi, however, both vertical distributions of currents (Figure 3a) and variations in thermohaline properties (Figure 2h) indicated upwelling-related changes in water column properties and coastal jets.

Table 1. Statistics of RDCEP measurements at Kõiguste and Matsi. Current speeds represent longshore currents; values which have negative northerly (i.e. a southerly) component, are shown as negative speeds

	Kõiguste	Matsi
measurement period	2 October 2010–11 May 2011	13 June–2 September 2011
data records [h]	5310	1941
depth range [m]	11.51–12.74	9.57–10.35
salinity range/average	4.72–5.9/5.50	4.72–5.55/5.21
temperature range	–0.38 ... 12.21	6.81 ... 21.71
average H_s wave height [m]	0.15	0.28
max. wave height [m]	2.93	2.46
gross average current speed [cm s ⁻¹]	5.3	7.3
max. near-bottom speed [cm s ⁻¹]	–21.9/21.4	–20.1/18.0
max. sub-surface speed [cm s ⁻¹]	–31.9/33.4	–34.4/26.5
mean/max. sustained wind [m s ⁻¹]	5.3/16.7	4.4/13.7
max. gust wind speed [m s ⁻¹]	25.6	19.0

It was discovered that, like the conditions on the Letipea Peninsula (Suursaar & Aps 2007, Suursaar 2010) and some other specific Baltic locations (e.g. Jankowski 2002, Leppäranta & Myrberg 2009), the straight coastal section near Matsi-Sõmeri is upwelling-prone when persistent northerly winds are blowing. Salinity increased and temperature decreased in summer (Figure 2h), and surprisingly high velocities were found in the surface layer. A baroclinic coastal jet was occasionally measured during the deployment of the instruments at Matsi (Figure 3a). Also, flow statistics (Figure 3b, Table 1) indicated that southward currents were faster even if the corresponding wind forcing was much weaker. The fastest SSE sub-surface current (34.4 cm s⁻¹, Table 1) occurred with a 4.6 m s⁻¹ wind blowing from the direction of 275°. The fastest NNW current (26.5 cm s⁻¹), however, was forced by a sustained 11.3 m s⁻¹ wind. On a small-scale map (e.g. Figure 1) the Kõiguste coast likewise seems relatively straight, but it actually has many small fjord-like bays, sub-marine shoals and islets, and no upwelling or upwelling-related coastal jets have been found there (Figure 2).

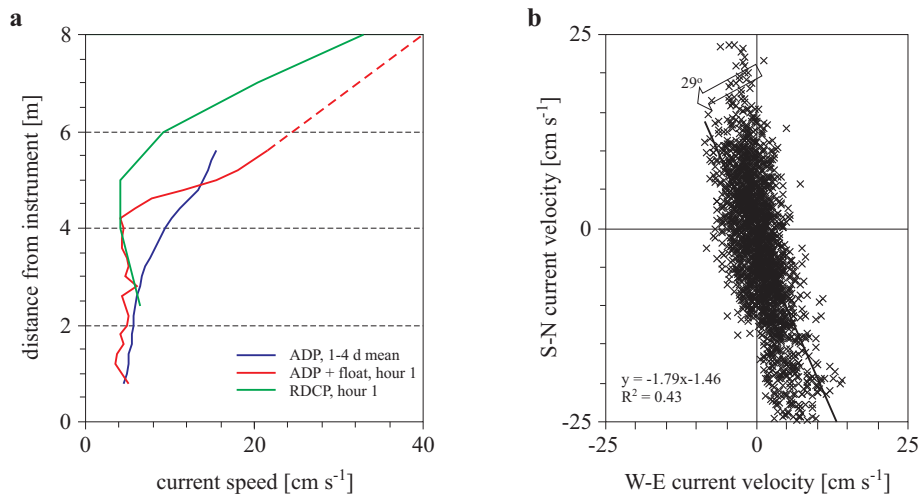


Figure 3. Measured vertical profiles of current speeds at Matsi (a). The data in the first hour on 13.06.2011 represent upwelling-related coastal jet conditions measured both by RDCP (depth 9.6 m) and ADP (depth 8 m), as well as by a Lagrangian surface float released at the time of ADP and RDCP deployments (average speed 39 cm s^{-1} during the first hour). Scatterplot of current velocity component values at Matsi at the depth layer 5–7 m from the bottom suggesting that the dominant flow direction is along the coast (b)

Throughout the measuring period, the average wave height at Kõiguste was relatively small due to ice cover, which either diminished fetch lengths or cut waves off altogether. However, in the first 80 days the average H_s was 0.39 m at Kõiguste and 0.28 at Matsi. As a result of restricted fetch lengths (approximately 150 km to SSE for Kõiguste and to SSW for Matsi) and the absence of severe storm conditions during the measurements, the maximum measured wave heights did not exceed 3 m (Table 1). The maximum H_s value was 1.63 m at Matsi and 1.96 m at Kõiguste, the energy wave periods peaked at 9.8 seconds at Kõiguste and 7.7 s at Matsi.

3.2. Calibration and validation of the models

Figure 4 compares (validates) the current velocity components measured at Matsi and those modelled with the 2D hydrodynamic model. The 2D model calculates the depth-averaged currents at the grid-points. The ‘measurements’ represent the time series of vertically averaged values over the depth range 2–9 m from the bottom. In addition, we assumed the vertical profile for the lowest 2 m would be constant and equal to the lowest measured cell until 1 m from the bottom, and that the bottom velocity would be zero. For the upper 2 m layer the profile was extrapolated up to the

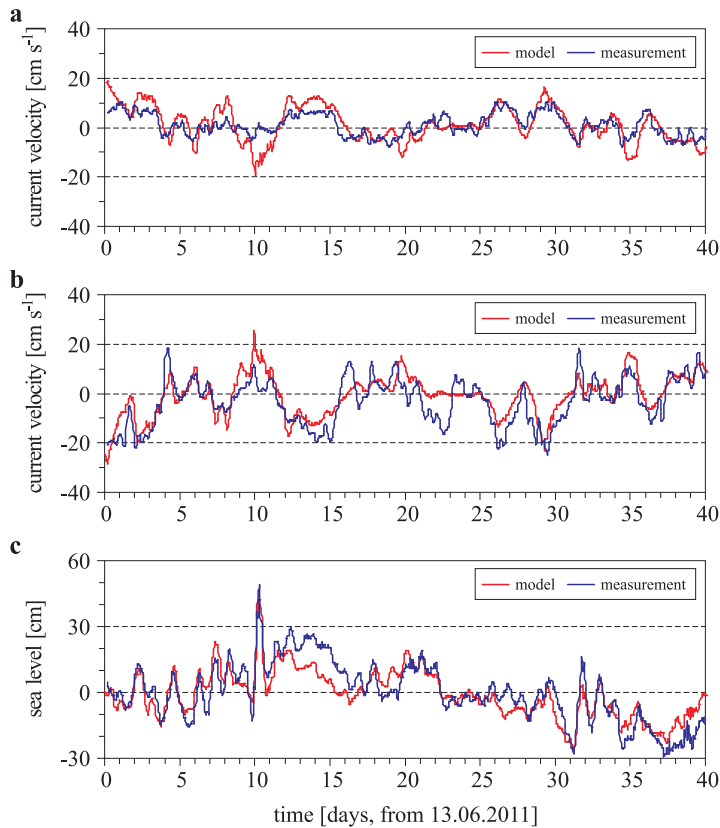


Figure 4. Comparison (validation) between the modelled and the measured velocities at Matsi: u -component (a) and v -component (b); sea level variations at Matsi (c; ‘measurement’ represents the RDCP depth values minus 9.9 m)

surface, depending on the uppermost measured cell, using the coefficients found in a procedure that minimizes the variance between the measured and modelled series over the full validation period. In general the velocity obtained over the vertical profile was slightly higher than the simple average of the measurements.

The comparison was performed at Matsi only. It was not possible to fully reproduce the rather complex micro-relief of the south-eastern coast of Saaremaa Island in the generalization with the 1 km grid-spacing of the model. As a result, the modelled currents at the ‘Kõiguste’ point showed prevailing longshore movements, whereas the actual measurements were more scattered.

At Matsi, both the modelled u and v velocity components (Figure 4a,b) showed rather good agreement with the measurements. The longshore, anti-clockwise rotated v -component (by 29 degrees, see also Figure 3b), which

was used later in the climatological scale hindcast, showed somewhat larger magnitudes as the respectively rotated u -component carried less variability. (However, this rotation itself did not improve the model's performance). As a 2D model inherently also simulates sea level variations, it was possible to validate the model against the RDCP measured sea level variations as well (Figure 4c). As a rule, proper hydrodynamic models do not need calibration, but the results can be controlled somewhat by the choice of coastline, bathymetry, cross-sections of the straits and wind input (Suursaar et al. 2002). We used un-modified Kihnu wind data, which represent the marine wind conditions over the Gulf of Riga, but may slightly overestimate the winds over the Väinameri. Bearing in mind further long-term hindcasts and the limited availability of hourly sea level data from earlier periods, we compared the simulations with the hourly sea level forcings taken from the Ristna tide gauge and interpolated from monthly average Ristna sea levels. The differences in cumulative current velocity components were surprisingly small (Figure 5a). The rather similar behaviour of the curves being compared can be explained by the use of integral data, where short-term fluctuations cancel each other out. Also, the study area is located in the central part of the model domain, where the high-frequency impulses of the boundary sea level conditions propagating from both the Irbe Strait and the Väinameri side meet each other. This means that the information carried by the high resolution wind forcing is the most important for currents (Otsmann et al. 2001), and low-frequency variations in boundary sea level are sufficient. Within the semi-enclosed sub-basins, their own sea level patterns are created by the model.

Unlike the 2D model, the SMB-type wave model is not a true hydrodynamic model and the results can be controlled (calibrated) somewhat by the depth-parameter, but more importantly by the choice of fetch lengths. Our calibrations included the depth-parameter of 19 m for Kõiguste and 21 m for Matsi. By trying to keep the maximum and average wave heights equal in the modelled and measured series (Figure 5b,c), which covered 40 days of hourly data at Kõiguste and 60 days at Matsi, maximizing the correlation coefficient and minimizing the RMSE, the best sets of fetches were obtained separately for Kõiguste and Matsi. Afterwards, using wind forcing from the same source (i.e. the Kihnu station) and the same fetches, long-term (1966–2011) wave hindcasts were calculated.

Because of the regular shape of the Gulf of Riga and the near absence of remotely generated wave components from the Baltic Proper, the calibrations were equally successful at Kõiguste and Matsi. Some mismatch between the measured and modelled time series (Figure 5) was due to

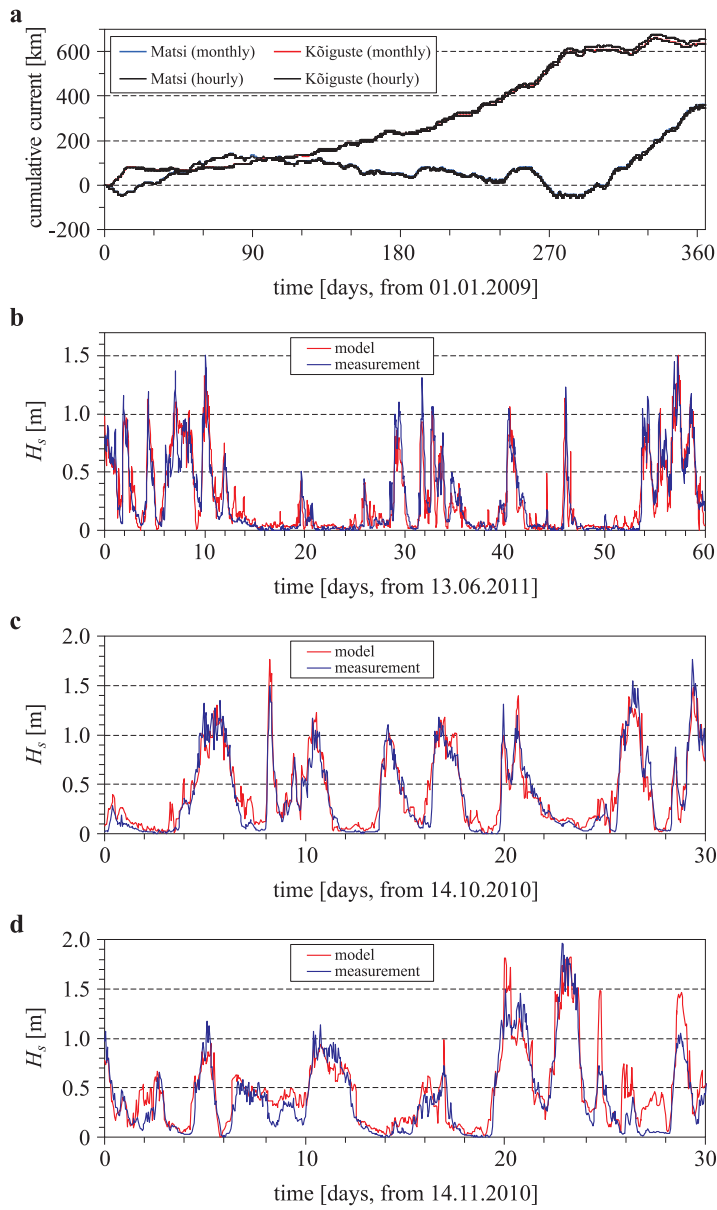


Figure 5. Comparison of cumulative longshore velocity components modelled with hourly and monthly open boundary sea level forcings at Ristna (a). Comparison between the measured and the modelled wave series at Matsi during the model calibration with Kihnu wind forcing (b) and a 30-day excerpt of calibration results at Kõiguste (c); validation of the wave model at Kõiguste on 14 November–14 December 2010 (d). In the few last days in (d) the influence of ice on the measurement series could be guessed

a temporal shift during strong wind events, and also as a result of local small-scale wind events, which do not spread over the 35–55 km distances between the wind forcing and modelling sites. In addition, a first-generation wave model cannot take into account gradual wave growth and subsiding (swell) features. The correlation coefficients between the hourly data series were 0.93 at Kõiguste and 0.91 at Matsi (960 and 1440 value pairs respectively). The RMSE was slightly better at Matsi (0.135 vs. 0.167 m). The RMSE, standardized with the variability range, which illustrates the prognostic value of the calibration, was 8.9% at Matsi and 9.4% at Kõiguste. These sets of comparative statistics were only marginally worse than in our previous experiences at the Harilaid Peninsula (Suursaar & Kullas 2009) and at Letipea (Suursaar 2010). The main reason for this was the absence of storm wave conditions and the relatively smaller range of values used in the calibration procedure. Strictly speaking, the calibration is fully valid for the conditions and variability range during the calibration. We can assume that on moving back from the calibration time, the results may get gradually worse.

Validation is possible when additional data sets of the same type are available outside the calibration periods. At Matsi, 60 days of relatively calm summer measurements were used in the calibration. But at Kõiguste in the autumn, apart from 40 days of calibration, some 30 days were left for validation just before sea-ice began to affect waves by shortening fetch distances. The validation results were very good (Figure 5d), r was 0.89 and the RMSE was equal to 0.197. Also, the validation (verification) we performed earlier at Letipea (see Figure 3 in Suursaar 2010) showed remarkably good agreement between measurements and calculations.

3.3. Current patterns and their relationships with wind forcing

Depending largely on morphometry, coastline and bottom topography, the current velocity components and sea surface height at every single point in the model domain possess a specific way of reacting to wind forcing. By choosing the points (of measurements) at Kõiguste and Matsi and applying the same methodology as Suursaar & Kullas (2006), the reaction of currents to wind direction can be investigated (Figures 6, 7). At Matsi, the strongest currents appeared in wind directions 150 and 330 degrees, and in 70 and 250 degrees at Kõiguste. However, when choosing a neighbouring, or just a different point, the result would be somewhat different as well (see Figure 6b).

In stationary or persistent wind forcing conditions, downwind flows prevail near the coasts of medium-size oval basins and large lakes, whereas

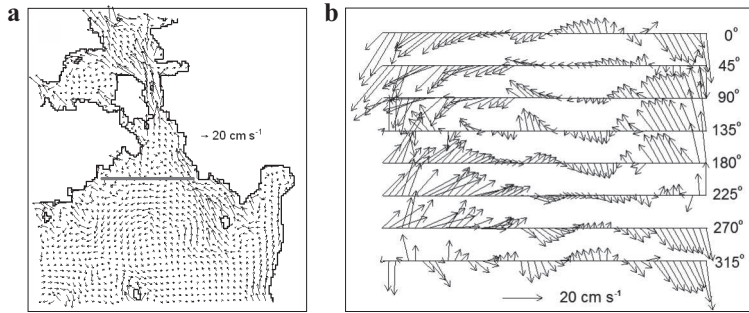


Figure 6. Typical flow patterns in the northern Gulf of Riga and the Archipelago Sea with stationary 10 m s^{-1} SE wind (a; every second arrow in the 1 km grid is drawn); dependence of velocity vectors on wind directions along the Kõiguste – Matsi section (b) with a 1 km grid step

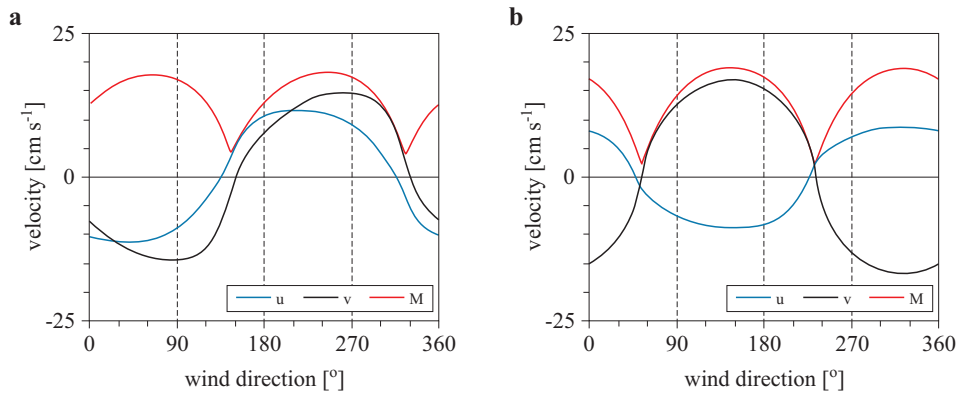


Figure 7. Modelled dependence between the direction of the stationary wind (10 m s^{-1}) and current velocity components (u , v , and moduli M) 3 km off Kõiguste (a) and 2 km off Matsi (b)

compensatory flows against the wind evolve along the deeper middle section of a sub-basin (Csanady 1973). For instance at Pärnu Bay, our simulations revealed two well-defined basin-scale flow regimes with cyclonic and anticyclonic circulation cells (Suursaar & Kullas 2006). The two wind directions which switch between the two regimes were approximately 120 and 300 degrees. Determined by the size and coastline, similar patterns were also found in simulations with stationary and uniform winds blowing from different directions in the northern Gulf of Riga (Figures 6, 7). The switching wind directions were approximately 90 and 270 degrees, differing slightly along the opposite coasts. In addition, the basin-wide circulation patterns are modified by the influence of the outlet-inlet of the Suur Strait.

The resulting patterns included several wave-like cycles (meanders or gyres), which shifted intricately when wind was slowly changing (Figure 6b). The wavelengths were as small as 5–6 km near the Saaremaa coast, but the patterns were more or less persistent at different wind speeds. Only minor alterations of wind speed occurred in the central part of the transect in wind directions blowing more or less along the transect (i.e. 90° , 135° , 270° and 315°). At the entrance to the 5–6 km wide Suur Strait, just two flow possibilities remained. All winds with a positive v -component elicited a northward current and a negative meridional wind component gave rise to a southward current. The direct influence of the Suur Strait flows was perceptible up to a distance of approximately 20 km into the northern Gulf. The influence of the Suur Strait on the basin-wide flow patterns was negligible with W and E winds.

3.4. Hindcast currents and wave conditions in 1966–2011

Although the models performed acceptably well, both in validation and in reproducing meso-scale hydrodynamic features, the ultimate goal of the study was a long-term hindcast. Simulated currents over 46 years demonstrated a large temporal variability. Typical velocities were 5–20 cm s^{-1} , but during extreme storms (e.g. in 1967, 1980, 2005) velocities up to 1 m s^{-1} were occasionally found. In an attempt to somehow summarize the huge amount of data and to describe climatological-scale variations, the cumulative longshore velocity components (Figure 8) as well as the cumulative flows through the cross-sections of the straits were calculated for each year. Despite the large scatter of conditions in individual years, the shapes of the whole ensembles as well as the average current trajectories indicated specific intra-annual patterns. At Kõiguste, the current was directed mostly north-westwards, faster in autumn and winter, slower in spring and summer (Figure 8a). At Matsi, northward flows were more probable in autumn and winter, southward flows were more likely in summer (Figure 8b). Plotting the last readings of each year against the year yielded time series like those on Figure 9.

As mentioned in connection with Figure 2, seasonal sea-ice can influence both currents and waves in the Gulf of Riga. There have been winters when there was no notable ice cover on the Gulf (e.g. 1988/89, 1989/90, 1991/92, 2001/02, 2007/08), but in a few winters the whole Gulf was fully ice-bound for 2–4 months. To eliminate such influences, parallel sets of cumulative currents were created, in which data from January to April were omitted, the annual series beginning equally on 1 May. Also, the summer months (May to August) were studied separately. However, it

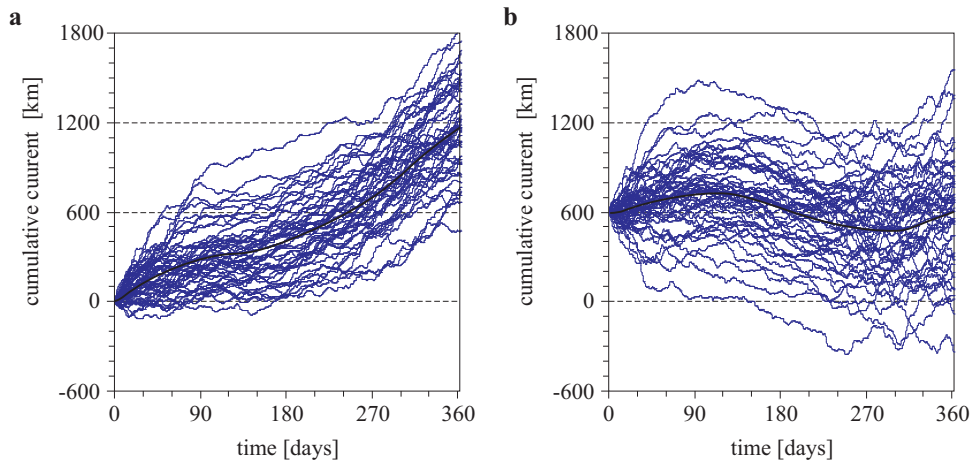


Figure 8. Annual (1966–2011) graphs of cumulative longshore currents at Kõiguste (a) and Matsi (b) plotted against the day of the year. The rotated compass direction 49° is positive in (a), and 331° in (b). The mean courses are shown with bold lines. See also Figure 5a for the course of a single year and Figures 9a,b, which represent the final values of the corresponding graphs in each year

appeared that the trends in shorter series remained nearly unchanged (Figure 9a–d).

In the straits, the annual sums of both individual in- and outflow could be as much as about 200 km^3 in the Suur and Hari Straits, and up to approximately 800 km^3 in the Irbe Strait (Otsmann et al. 2001). As expected from previous studies (Suursaar et al. 1995, Astok et al. 1999, Raudsepp et al. 2011), our results of cumulative fluxes also indicated an annual net outflow in the Suur Strait. The northward fluxes (on average approximately $60 \text{ km}^3 \text{ yr}^{-1}$) were somewhat larger than those calculated by Raudsepp et al. (2011) for 2008 ($23 \text{ km}^3 \text{ yr}^{-1}$). The difference could have occurred for several reasons. Firstly, Raudsepp et al. (2011) admitted that their (single-point) measuring site, which was at the depth of 3.5 m on one side of the strait, might not fully represent the whole cross section. Also, the wind stress from the HIRLAM (High Resolution Limited Area Model) could have underestimated the winds above the narrow strait, as the corresponding model cells probably included land surface properties. On the other hand, as indicated by the long-term average wind speed at Kihnu (5.66 m s^{-1} in 1966–2011 vs. 4.15 m s^{-1} at Virtsu), our forcing may have overestimated the winds above the Väänameri part of the model domain. Finally, unlike Raudsepp et al. (2011), our calculations included constant $32 \text{ km}^3 \text{ yr}^{-1}$ inflows from rivers into the Gulf of Riga. (The seasonal variations in discharges have been largely controlled by the Riga

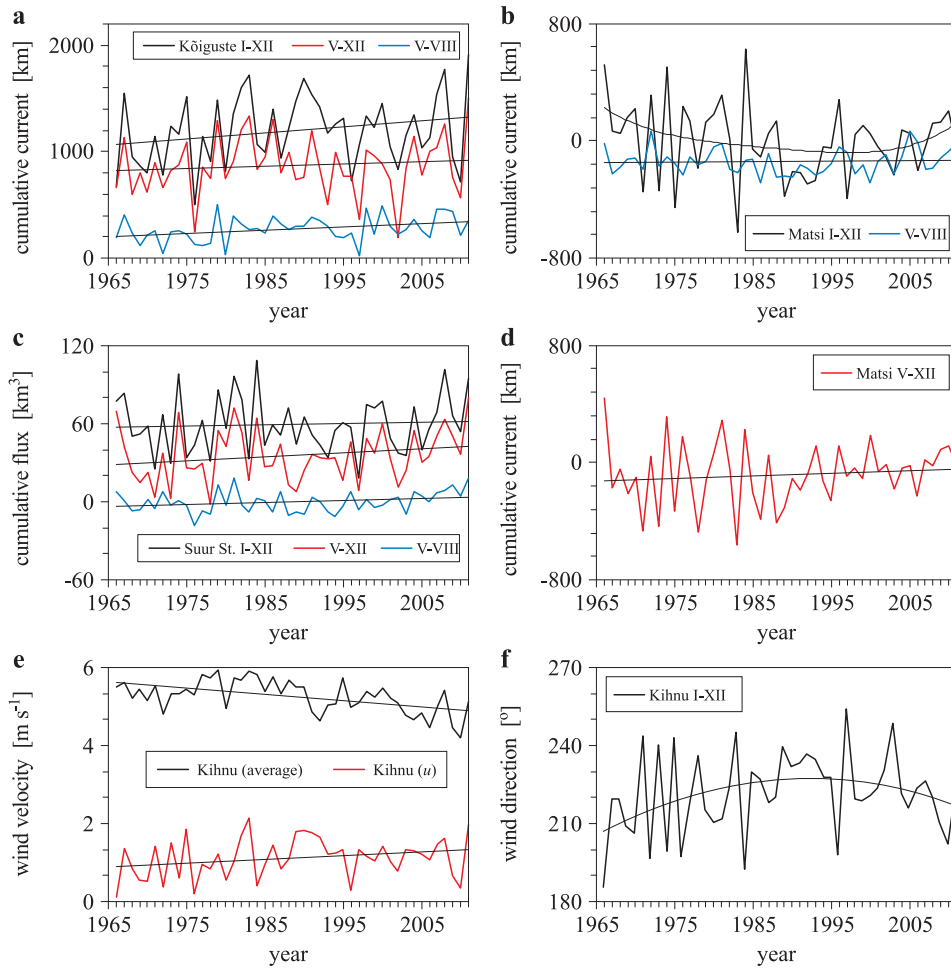


Figure 9. Variations in annual cumulative longshore currents at Kõiguste (a; NE is positive) and Matsi (b,d; NNW is positive) in different parts of the year (full year, winter months excluded, only summer months included), cumulative fluxes through the Suur Strait (c; N is positive), annual Kihnu mean wind speed and *u*-components (e), and resultant wind directions at Kihnu (f)

Hydroelectric Power Plant on the River Daugava since 1974.) Although the larger part of that discharge ought to ‘flow out’ through the Irbe Strait, no one has any certain knowledge of the actual proportion. In general, the inflow through the Irbe Strait should mirror the outflow through the Suur Strait, but in the relatively wide Irbe Strait under certain conditions in- and outflow can take place simultaneously (Lilover et al. 1998). The question could probably be solved either by studying Lagrangian particle tracks (like Zhurbas et al. (2010) did in the Baltic Proper), or water

‘age’ (see e.g. Andrejev et al. 2004). Summarizing the problem for the Gulf of Riga, the interannual proportions as well as climatological shifts should remain the same, even though the exact magnitude of flows is unknown.

Being differently exposed (Kõiguste to SE, Matsi mostly to S-SW), the locations showed a rather different wave time series (Figure 10). According to formal linear trends, the average wave heights have probably decreased at both locations. While at the windward Matsi the overall linear trend decreased very slightly in 1966–2011, the trend was a significantly falling one near Kõiguste (Figure 10a). However, on the basis of annual maxima and higher quantiles (90%, 99%), the trends increased near Matsi, but still decreased near Kõiguste (Figure 10c,d). Especially at Matsi, the wave heights showed some quasi-periodic cycles with high stages in 1980–1995 and again after about 2007. The cycles basically followed those in atmospheric processes (Figure 9; Jaagus et al. 2008). Cutting off the data from the first four months of the year did not alter the results very much, as the average wave heights in May–August were the lowest (Figure 10c), in September–December the highest, and in January to April around average.

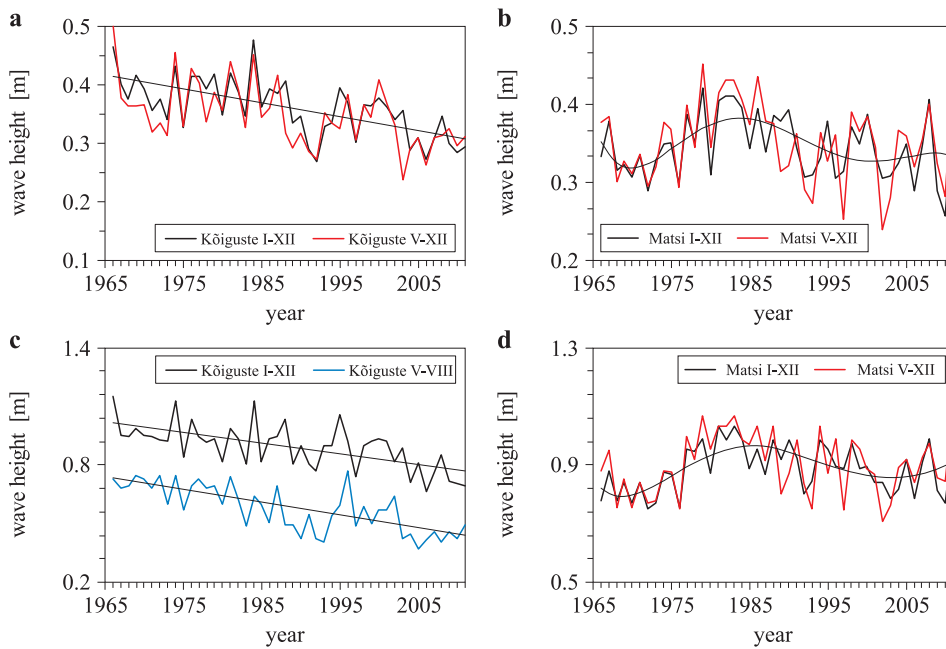


Figure 10. Variations in annual mean wave heights (a,b), and 90-percentile wave heights (c,d) at Kõiguste and Matsi computed over different periods of the year in 1966–2011

3.5. Relationships of currents, waves and water exchange with changes in wind climate

Despite the decrease in Kihnu mean wind speed (Figure 9e), currents have increased slightly both at Kõiguste and in the Suur Strait (Figure 9a,c). The possible reason is the increase in the westerly (u) component of winds (Figure 9e), which clearly controls the currents at Kõiguste. The correlation coefficient between the longshore current and the Kihnu wind u -component was as high as 0.91 (0.57 in the case of the v -component and 0.86 in mean wind speed). Fluxes in the Suur Strait probably increased because more water was pushed into the Gulf through the Irbe Strait, which in turn should flow out (northwards) through the Suur Strait and finally through the Hari Strait, as the smaller Soela Strait contributes with net inflows as well (Figures 1, 6a). Yet the fluctuations in the cumulative fluxes in the Suur Strait were better described by the v component of the Kihnu wind ($r=0.92$).

At Matsi, the trend depended on season (Figure 9b,d) and the current direction depended on the wind direction (which tends to be nearly perpendicular to the coast; Figure 9f). Interestingly enough, the cumulative currents at Matsi had a strong connection ($r=-0.94$) with the Kihnu wind direction with respect not only to flow directions but also to current magnitudes. The wave time series at the westerly exposed Matsi were more or less level (or slightly increasing in the case of higher percentiles, Figure 10d) as the westerly wind component increased (Figure 9e). Waves at Kõiguste have decreased because the average wind, but also easterly and southerly wind speeds, have also been decreasing.

The spatially contrasting results for coastal sections with westerly and southerly-easterly exposures were probably related to the changes in atmospheric pressure patterns above northern Europe and the poleward shift of cyclone trajectories in recent decades (Pinto et al. 2007, Jaagus et al. 2008, Lehmann et al. 2011). As far as waves are concerned, it is important that there were more cyclones, which by-passed Estonia to the north, creating strong westerly winds (Suursaar 2010). The tendencies in winds blowing from directions with longer fetches are far more important than in winds with short fetches. The prevailing overall decrease in mean wave properties, the increase in high wave events at selected locations of the Estonian coastal sea, and their relationship with wind regimes was already noted in 2009–2010 (Suursaar & Kullas 2009, Suursaar 2010, Soomere & Räämet 2011). Although no long-term wave hindcasts existed for the Gulf of Riga, in other parts of the Estonian coastal sea different models and methods deliver somewhat different results in specific details (Broman et al. 2006, Räämet et al. 2009, Suursaar 2010).

The modelling results always depend on the quality or specific properties of the forcing data. In the case of routinely measured wind data, instrument changes or long-term gradual changes in land use and surface roughness may lead to inhomogeneities and uncertainties in long-term wave hindcasts, too. Closely related to the observed large-scale variations in atmospheric conditions (Pinto et al. 2007), including the NAO (Suursaar & Sooäär 2007), the general patterns both in wave and wind statistics are probably valid. The Kihnu station has always been in relatively open terrain. Regarding changes in instrumentation (see also ‘Material and methods’), the forcing data were probably more or less homogeneous in 1966–2011, or at least it was in 1976–2011 (Keevallik et al. 2007). Yet the possible specific influences of these factors should be further addressed by climatologists and meteorologists.

4. Conclusions

Based on high quality measurements of waves and currents obtained with a bottom-mounted RDCP at two differently exposed locations (Kõiguste to SE and Matsi to SW) for a total duration of 302 days, and long-term simulations of currents and water exchange using the Gulf of Riga-Väinameri 2D hydrodynamic model, typical flow patterns and climatologically related changes in hydrodynamic conditions were studied. Using wind forcing data from the Kihnu meteorological station, a set of current, water exchange and wave hindcasts were obtained for the period 1966–2011.

Current patterns in the Gulf and in the straits were wind-dependent with characteristic switch directions for each location. The Matsi coast is prone to upwelling in persistent northerly wind conditions, whereas the Kõiguste coast is not conducive to upwelling events. At Kõiguste, the current was directed mostly to NW, faster in autumn and winter, and slower in spring and summer. At Matsi, northward flows were more probable in autumn and winter and southward flows in summer. Currents have increased along the Kõiguste coast and in the Suur Strait. According to the hindcast, which took into account freshwater inflow to the Gulf of Riga but did not consider variations in real ice conditions, a net outflow ($20\text{--}110\text{ km}^3\text{ yr}^{-1}$) prevailed in the Suur Strait.

A fetch-based calibration scheme for simple wave models with good comparison results was applied, and hindcasts as ‘extensions of in situ measurements’ at the two differently exposed locations in the Gulf of Riga were performed. The hindcast results showed some quasi-periodic cycles with high stages in 1980–1995 and also after 2007, a prevailing overall decrease in mean wave properties, an increase in high wave events in windward locations, and their relations with wind regimes. The spatially

contrasting results for westerly and northerly-easterly exposed coastal sections are probably related to the changes in atmospheric pressure patterns above northern Europe and the poleward shift of cyclonic trajectories.

Acknowledgements

The authors are grateful to the Estonian Meteorological and Hydrological Institute for providing meteorological and sea level data, and to Dr Georg Martin, Kaire Kaljurand and Arno Põllumäe for helping with the RDCP mooring.

References

- Andrejev O., Myrberg K., Alenius P., Lundberg P., 2004, *Mean circulation and water exchange in the Gulf of Finland – a study based on three-dimensional modelling*, Boreal Environ. Res., 9 (1), 1–16.
- Astok V., Otsmann M., Suursaar Ü., 1999, *Water exchange as the main physical process in semi-enclosed marine systems: the Gulf of Riga case*, Hydrobiologia, 393 (0), 11–18, <http://dx.doi.org/10.1023/A:1003517110726>.
- Berzins V., Bethers U., Sennikovs J., 1994, *Gulf of Riga: bathymetric, hydrological and meteorological databases, and calculations of the water exchange*, Proc. Latvian Acad. Sci., B7/8, 107–117.
- Bowman M. J., Esaias W. E. (eds.), 1978, *Oceanic fronts in coastal processes*, Springer-Verlag, Berlin, 114 pp.
- Broman B., Hammarklint T., Rannat K., Soomere T., Valdmann A., 2006, *Trends and extremes of wave fields in the north-eastern part of the Baltic Proper*, Oceanologia, 48 (S), 165–184.
- Csanady G. T., 1973, *Wind-induced barotropic motions in long lakes*, J. Phys. Oceanogr., 3, 429–438, [http://dx.doi.org/10.1175/1520-0485\(1973\)003<0429:WIBMIL>2.0.CO;2](http://dx.doi.org/10.1175/1520-0485(1973)003<0429:WIBMIL>2.0.CO;2).
- Huttula T., 1994, *Suspended sediment transport in Lake Säkylän Pyhäjärvi*, Aqua Fenn., 24 (2), 171–185.
- Jaagus J., Post P., Tomingas O., 2008, *Changes in storminess on the western coast of Estonia in relation to large-scale atmospheric circulation*, Climate Res., 36 (1), 29–40, <http://dx.doi.org/10.3354/cr00725>.
- Jankowski A., 2002, *Variability of coastal water hydrodynamics in the southern Baltic – hindcast modelling of an upwelling event along the Polish coast*, Oceanologia, 44 (4), 395–418.
- Jones J. E., Davies A. M., 2001, *Influence of wave-current interaction, and high frequency forcing upon storm induced currents and elevations*, Estuar. Coast. Shelf Sci., 53 (4), 397–413, <http://dx.doi.org/10.1006/ecss.1999.0622>.
- Jönsson A., 2006, *A model study of suspended sand due to surface waves during a storm in the Baltic Proper*, J. Marine Syst., 63 (3–4), 91–104, <http://dx.doi.org/10.1016/j.jmarsys.2006.05.005>.

- Keevallik S., Soomere T., Pärj R., Zhukova V., 2007, *Outlook for wind measurements at Estonian automatic weather stations*, Proc. Estonian Acad. Sci.-Eng., 13 (3), 234–251.
- Kotta J., Paalme T., Püss T., Herkül K., Kotta I., 2008, *Contribution of scale-dependent environmental variability on the biomass patterns of drift algae and associated invertebrates in the Gulf of Riga, northern Baltic Sea*, J. Marine Syst., 74 (Suppl. 1), S116–S123, <http://dx.doi.org/10.1016/j.jmarsys.2008.03.030>.
- Kovtun A., Torn K., Martin G., Kullas T., Kotta J., Suursaar Ü., 2011, *Influence of abiotic environmental conditions on spatial distribution of charophytes in the coastal waters of West Estonian Archipelago, Baltic Sea*, J. Coastal Res., SI64 (1), 412–416.
- Kullas T., Otsmann M., Suursaar Ü., 2000, *Comparative calculations of flows in the straits of the Gulf of Riga and the Väinameri*, Proc. Estonian Acad. Sci. Eng., 6 (4), 284–294.
- Lehmann A., Getzlaff K., Harlass J., 2011, *Detailed assessment of climate variability in the Baltic Sea area for the period 1958 to 2009*, Climate Res., 46 (2), 185–196, <http://dx.doi.org/10.3354/cr00876>.
- Leppäranta M., Myrberg K., 2009, *Physical oceanography of the Baltic Sea*, Springer Praxis, Berlin–Heidelberg–New York, 378 pp.
- Lilover M. J., Lips U., Laanearu J., Liljebadh B., 1998, *Flow regime in the Irbe Strait*, Aquat. Sci., 60 (3), 253–265, <http://dx.doi.org/10.1007/s000270050040>.
- Luhamaa A., Kimmel K., Männik A., Rõõm R., 2011, *High resolution re-analysis for the Baltic Sea region during 1965–2005 period*, Clim. Dynam., 36 (3–4), 727–738, <http://dx.doi.org/10.1007/s00382-010-0842-y>.
- Massel S. R., 1996, *Ocean surface waves: their physics and prediction*, World Sci., Singapore, 491 pp., <http://dx.doi.org/10.1142/9789812795908>.
- Ojaveer E., 1995, *Ecosystem of the Gulf of Riga between 1920 and 1990*, Academia 5, Estonian Acad. Publ., Tallinn, 272 pp.
- Otsmann M., Astok V., Suursaar Ü., 1997, *A model for water exchange between the Baltic Sea and the Gulf of Riga*, Nord. Hydrol., 28 (4–5), 351–364.
- Otsmann M., Suursaar Ü., Kullas T., 2001, *The oscillatory nature of the flows in the system of straits and small semi-enclosed basins of the Baltic Sea*, Cont. Shelf Res., 21 (15), 1577–1603, [http://dx.doi.org/10.1016/S0278-4343\(01\)00002-4](http://dx.doi.org/10.1016/S0278-4343(01)00002-4).
- Pinto J. G., Ulbrich U., Leckenbusch G. C., Spangehl T., Reyers M., Zacharias S., 2007, *Changes in storm track and cyclone activity in three SRES ensemble experiments with the ECHAM5/MPI-OM1 GCM*, Clim. Dynam., 29 (2–3), 195–210, <http://dx.doi.org/10.1007/s00382-007-0230-4>.
- Raudsepp U., Laanemets J., Haran G., Alari V., Pavelson J., Kõuts T., 2011, *Flow, waves and water exchange in the Suur Strait, the Gulf of Riga in 2008*, Oceanologia, 53 (1), 35–56, <http://dx.doi.org/10.5697/oc.53-1.035>.
- Räämet A., Suursaar Ü., Kullas T., Soomere T., 2009, *Reconsidering uncertainties of wave conditions in the coastal areas of the northern Baltic Sea*, J. Coastal Res., Sp. Iss. (56), 257–261.

- Scientific-practical handbook of the climate of the U.S.S.R.*, 1990, Part 3, Gidrometeoizdat, Leningrad, (in Russian).
- Seymour R. J., 1977, *Estimating wave generation in restricted fetches*, J. Waterw. Port. C. Div., 103 (WW2), Paper No. 12924, 251–263.
- Smith S. D., Banke E. G., 1975, *Variations of the sea surface drag coefficient with wind speed*, Q. J. Roy. Meteorol. Soc., 101, 665–673, <http://dx.doi.org/10.1002/qj.49710142920>.
- Soomere T., 2003, *Anisotropy of wind and wave regimes in the Baltic proper*, J. Sea Res., 49 (4), 305–316, [http://dx.doi.org/10.1016/S1385-1101\(03\)00034-0](http://dx.doi.org/10.1016/S1385-1101(03)00034-0).
- Soomere T., Räämet A., 2011, *Long-term spatial variations in the Baltic Sea wave fields*, Ocean Sci., 7 (1), 141–150, <http://dx.doi.org/10.5194/os-7-141-2011>.
- Suursaar Ü., 2010, *Waves, currents and sea level variations along the Letipea – Sillamäe coastal section of the southern Gulf of Finland*, Oceanologia, 52 (3), 391–416, <http://dx.doi.org/10.5697/oc.52-3.391>.
- Suursaar Ü., Aps R., 2007, *Spatio-temporal variations in hydro-physical and -chemical parameters during a major upwelling event off the southern coast of the Gulf of Finland in summer 2006*, Oceanologia, 49 (2), 209–228.
- Suursaar Ü., Astok V., Kullas T., Nõmm A., Otsmann M., 1995, *Currents in the Suur Strait and their role in the nutrient exchange between the Gulf of Riga and the Baltic Proper*, Proc. Estonian Acad. Sci. Ecol., 5 (3/4), 103–123.
- Suursaar Ü., Kullas T., 2006, *Influence of wind climate changes on the mean sea level and current regime in the coastal waters of west Estonia, Baltic Sea*, Oceanologia, 48 (3), 361–383.
- Suursaar Ü., Kullas T., 2009, *Decadal variations in wave heights off Kelba, Saaremaa Island, and their relationships with changes in wind climate*, Oceanologia, 51 (1), 39–61, <http://dx.doi.org/10.5697/oc.51-1.039>.
- Suursaar Ü., Kullas T., Otsmann M., 2002, *A model study of the sea level variations in the Gulf of Riga and the Väinameri Sea*, Cont. Shelf Res., 22 (14), 2001–2019, [http://dx.doi.org/10.1016/S0278-4343\(02\)00046-8](http://dx.doi.org/10.1016/S0278-4343(02)00046-8).
- Suursaar Ü., Kullas T., Otsmann M., Saaremäe I., Kuik J., Merilain M., 2006, *Cyclone Gudrun in January 2005 and modelling its hydrodynamic consequences in the Estonian coastal waters*, Boreal Environ. Res., 11 (2), 143–159.
- Suursaar Ü., Sooäär J., 2007, *Decadal variations in mean and extreme sea level values along the Estonian coast of the Baltic Sea*, Tellus A, 59 (2), 249–260, <http://dx.doi.org/10.1111/j.1600-0870.2006.00220.x>.
- Tõnisson H., Orviku K., Jaagus J., Suursaar Ü., Kont A., Rivis R., 2008, *Coastal damages on Saaremaa Island, Estonia, caused by the extreme storm and flooding on January 9, 2005*, J. Coastal Res., 24 (3), 602–614, <http://dx.doi.org/10.2112/06-0631.1>.
- USACE – U.S. Army Corps of Engineers, 2002, *Coastal engineering manual*, Rep. EM 1110-2-1100, U.S. Govt. Print. Office, Washington DC.

Zhurbas V., Elken J., Väli G., Kuzmina N., Paka V., 2010, *Pathways of suspended particles transport in the bottom layer of the southern Baltic Sea depending on wind forcing (numerical simulations)*, *Oceanology*, 50 (6), 841–854, doi:10.1134/S0001437010060032.